Egyptian Journal of Chemistry

http://ejchem.journals.ekb.eg/

Different studies on the interaction of Lead nitrate salt with Orange G

Mohamed Fathi[1]*, Hamada M. Killa[1], Esam A. Gomaa[2], Shereen E. Salem[2], A.Farouk[1]

[1) *Chemistry Department, Faculty of Science, Zagazig University, Egypt.*

[2) *Chemistry Department, Faculty of Science, Mansoura University, Egypt.*

Abstract

For lump lead nitrate (Pb (NO3)2) in pure water, the affiliation and thermodynamic association characteristics were assessed at 298.15, 303.15, 308.15, and 313.15K. based on the lump Pb(NO3)2 molar conductance, Estimates were made for the parameters of the solvation, such as the activity coefficient, enthalpy of association, free energy of association, association constant and entropy of association. From the interaction of bulk Pb(NO3)2 with Orange G. There were two stoichiometric complexes produced. 1:1 and 1:2 In the case of 1:1 (Pb(NO3)2/ Orange G) compared to 1:2 (Orange G in pure water as solvent), the complex Kf and ΔGf are higher, indicating simpler complex formation. Temperature increase resulted in a drop in the formation constants. The complexation's negative ΔGf values demonstrate that the process of complex synthesis was spontaneous and that the temperature improved the spontaneity. Finally , Orange G and its lead complex with the crystalline structure for the human prostate specific antibody (PSA) in a Fab sandwich have been subjected to molecular docking with a high affinity. Utilizing Docking Server software, Gaussian 09, DS Biovia Material Studio 2017, Material Studio 07.0, and molecular modelling and computational computations were completed

Keywords: Orange G, Lead nitrate salt, Conductometry, Association and Thermodynamic parameters, Molecular docking, Human prostate specific antigen (PSA).

1. Introduction

An electrolyte solution's conductivity is an indication of how well it conducts electricity. Siemens per meter (S/m) is the SI unit for conductivity [1,2]. The number of ions in a solution may be quickly, cheaply, and accurately determined using conductivity measurements in various industrial and environmental applications [3-5]. For instance, one common technique for monitoring changes in the effectiveness of water purification systems over time is the measurement of product conductivity. One of the most precise physical methods for evaluating the electrolyte of solutions is conductance measurement [6,7]. Measurements of conductivity are commonly utilized in industry. Water treatment is one of the most crucial applications since untreated water from a lake, river, or a pipe is usually ineffective for industrial usage. If the contaminants in the water are not removed, they will cause corrosion and scale in the plant's machinery, especially in the boilers, cooling towers, and heat exchangers. There are numerous methods for treating water, and each one has a unique purpose. Demineralization, or the elimination of all or almost all contaminants, is frequently the intended outcome. In some instances, the intention is to eliminate only a certain contaminant, such as hardness ions (calcium and magnesium). Since conductivity measures the entire ion concentration [8 , 9]. analyzing complexation processes in various solvent formulations and interpreting them in terms of the solute being solvated preferentially by a component of the solvent [10–12]. In this work, Calculations of conductivity were done utilizing lump $Pb(NO_3)_2$ in H_2O in the lack and in the presence of Orange G. lead compounds have received a lot of attention lately because they perform a big part in a lot of biochemical processes and are used in so many various industries including industrial and medicinal chemistry [13–16].

Antibiotics, often known as antibacterials, are antimicrobial drugs that are used to treat and prevent bacterial infections. These compounds may kill or inhibit bacteria. Only a few antibiotics have antiprotozoal activity [17]. The characteristic azo dye Orange G (OG), found in textile greywater, has been the subject of 75 in-depth studies. The Papanicolaou stain colours keratin using Orange G. It plays a significant role in the pollen staining Alexander test as well. In the trichrome methods, it is typically used with some other yellow dye to stain erythrocytes. [18,19,20].

Using Docking Server, allows docking calculations to be carried out on the Orange G protein model [21]. Rotatable bonds; were defined, merging the non-polar hydrogen atoms and adding Gasteiger partial charges to the atoms of the ligand, by using the AutoDock tools also; Additional information was provided regarding the solvation parameters, Kollman unity atom type charges, and necessary hydrogen atoms. [22].

2. Experimental work

2.1. Materials and Solvents

Pure lead nitrate salt [Pb(NO₃)₂] supplied Sigma, Orange G (OG) from Ranken Lab, isolated potassium chloride salt (KCl) from Sigma-Aldrich, and improved water generated with a specified conductivity of 4.1 μS cm^{-1} were the compounds employed in the current study.

Orange G (OG)
(disodium;7-hydroxy-8-phenyldiazenylnaphthalene-1,3-disulfonate

Formula	$C_{16}H_{10}N_2Na_2O_7S_2$
Mol. wt.	452.38 g/mol

2.2. Conductance measurements

The conductance of a lead nitrate solution, pb(NO₃)₂ (10^{-3} M), was measured while a titration cell containing the solution was thermostated at a specified temperature. A precalibrated micropipette was used to quantify the conductivity of the mixture after each transfer of the Orange G ligand (10^{-4} M) to the titration cell. Up until the overall ligand concentration was around four times greater than the total concentration of metal ions, the ligand solution was added continuously. After each addition, the solution's conductivity was assessed. Applying computer fitting to the molar conductance mole ratio data, We studied the molar conductance of the complex ML as well as the complex formation constant Kf.Temperatures (298.15, 303.15, and 308.15) are employed. After each addition, the solution's conductance was gauged. Through computer fitting to the molar conductance mole ratio data, the complex formation constant Kf and the molar conductance of the complex ML were assessed. (298.15, 303.15, 308.15, and 313.15) K are the used temperatures. An ultra-thermostat of the Kottermann 4130 type was used to maintain the temperature constant at the proper value with 0.004 °C of variance in order to obtain the specific conductivity Ks with a cell constant of 1.04 cm^{-1} and (0.1 S cm^{-1}) of a variance. Solutions containing potassium chloride were employed to calibrate the cell.

2.3. Molecular Docking

It was decided to use the Molecular Operating Environment (MOE) to illustrate why certain chemicals have antiviral activity. The structural model was constructed using the MOE BUILDER module, and in a two-step procedure, optimization conformational evaluations of the produced molecules were performed. First, the semiempirical PM3 Hamiltonian with Restricted Hartree-Fock (RHF) and an RMS gradient of 0.05 Kcal/mol was used to optimize the geometry of these compounds. This was done using the integrated MOPAC 7.0 energy minimization tool. The generated model was then applied to the MOE's "Systematic Conformational Search.".

Orange G and its lead complex with the crystal structure of the human prostate specific antigen (PSA) in Fab sandwich had been subjected to molecular docking with a high affinity. Utilizing molecular modelling and computational computations were completed.

3. Results and Discussion

3.1. Estimation of thermodynamic parameters using conductometric measurements.

The quantity and kind of donor atoms, as well as the size and number of chelate rings generated during complexation, and other variables all affect how stable a transition metal complex is with a polydentate chelate ligand [23-24].

In many dye compounds used in histology, Orange G is a synthetic azo dye. The most common form is as a disodium salt. It resembles orange crystals or powder in appearance. Despite having two ionizable groups, it only exhibits vivid orange in neutral and acidic pH ranges or red in pH ranges above 9[25-27].

3.1.1. estimation of association constants and thermodynamic parameters for lead nitrate [pb(NO3)2] with pure water [H2O] in absence of ligand [Orange G, OG].

Experimental measurements were made to determine the specific conductance values (K_s) of various concentrations of $pb(NO_3)_2$ in H_2O in the lacking of OG at various temperatures (298.15, 303.15, 308.15, and 313.15)K. The values of molar conductance (Λ_m) were computed [28–29]. Utilizing formula (1):

$$\Lambda_m = \frac{(K_s - K_{solv})K_{cell} \times 1000}{C} \quad (1)$$

where K_{cell} is the cell constant, C is the molar concentration of the $pb(NO_3)_2$ solution, and K_s and K_{solv} are the specific conductance of the solution and the pure water solution, alternately.

For $pb(NO_3)_2$ with H_2O in the absence of OG at various temperatures, the limiting molar conductance (Λ_0) at infinite dilutions were calculated by extending the relation among Λ_m agonist $C_m^{1/2}$ to zero concentration as shown in **Fig.2.**
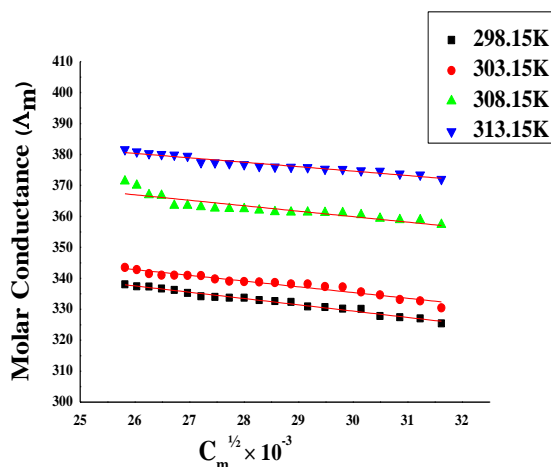
Fig.2: The relationship among molar conductance (Λ_m) and ($C_m^{1/2}$) of $pb(NO_3)_2$ in H_2O at various temperatures.

Fuoss-Shedlovsky was used to assess the experimental conductance measurement data [30-31]. Extrapolation methods that are used after equation (2–12): -

$$\frac{1}{\Lambda S_{(Z)}} = \frac{1}{\Lambda_o} + \left(\frac{K_A}{\Lambda_o^2}\right)\left(C\Lambda\gamma_\pm^2 S_{(Z)}\right) \quad (2)$$

where, $S_{(Z)} = 1 + Z + Z^2/2 + Z^3/8 + \ldots$ etc. and

$$Z = \frac{S(\Lambda C)^{1/2}}{\Lambda_o^{3/2}} \quad (3)$$

The Onsager slope (S) was computed from the equation (4) by using the value of (Λ_0):

$$S = a\Lambda_0 + b \quad (4)$$

where, $a = 8.2 \times 10^5 /(\varepsilon T)^{3/2} \quad (5)$

$b = 82.4/\eta((\varepsilon T)^{1/2} \quad (6)$

where (ε) denotes the solvent's dielectric constant, (η_0) its viscosity, and (T) its temperature.

Equation (7) was employed to determine the amounts of the degree of dissociation (α):

$$(\alpha) = \Lambda S_{(Z)} / \Lambda_0 \quad (7)$$

Equation (8) was used to estimate the average activity coefficients ($\gamma_\pm$).

$$\log \gamma_\pm = - A(\alpha C)^{1/2} / [1+B\,r^o(\alpha C)^{1/2})] \quad (8)$$

where, ($z^- z^+$) are the charges of ions in solutions A, B are the Debye-Hückel constant.

$A = 1.824 \times 10^6 (\varepsilon T)^{-3/2}$; $B = 50.29 \times 10^8 (\varepsilon T)^{-1/2}$ and (r^o) is the solvated radius.

Formula (9) gives the association constant (K_A):

$$K_A = \frac{C_{[MX_n]} \cdot \gamma_{[MX_n]}}{C_{M^{n+}} \cdot \gamma_{M^{n+}} \cdot C_{X^-}^n \cdot \gamma_{X^-}^n} \quad (9)$$

Equation (10) can be used to quickly determine the amounts of the dissociation constant (K_D) utilizing the relationship constant values (K_A)

$$K_D = 1/K_A \quad (10)$$

The quantities of the triple ion association constant (K_3) were computed [32-33].by utilizing the formula (11):

$$\frac{\Lambda C^{1/2}}{(1-\frac{\Lambda}{\Lambda_o})^{1/2}} = \frac{\Lambda_o}{(K_A)^{1/2}} + \frac{\lambda_3^o C}{K_3(K_A)^{1/2}}(1 - \frac{\Lambda}{\Lambda_o}) \quad (11)$$

The Walden assumption ($\Lambda_0 = 3\lambda_0$) was used by Fuoss [34] to construct equation (11).

At different temperatures (298.15, 303.15, 308.15, and 313.15)K, the quantities of the free energy of association (ΔG_A) of $pb(NO_3)_2$ in H_2O were

computed [35-36]. from the quantities of the association constant (KA) applying equation (12).

$$\Delta G_A = -2.303\ RT \log K_A \qquad (12)$$

where, R is the gas constant (8.314 J.mol^{-1} degree^{-1}) and T is the absolute temperature. The computed quantities of $S_{(Z)}$, $\gamma_\pm$, K_A, K_D, α, K_3 $\eta_{0'}$ $\Lambda_{0'}$ Λ_m, C, S, Z, and Gibbs free energies for the solutions of pb(NO$_3$)$_2$ in H$_2$O at various temperatures (298.15, 303.15, 308.15 and 313.15)K were obtained and listed in **Table.1.**

Table (1): various solvation parameters: K$_A$, K$_D$ and K$_3$ of lump pb(NO$_3$)$_2$ in solvent H$_2$O in lack of orang G.

Temperature. (K)	10^2 η_o (poise)	Λ_m	Λ_0	S	Z	$S_{(z)}$	$\gamma_\pm$	α	K_A	10^3 K_D	10^5 K_3	ΔG_A
298.15	0.8903	327.05	376.16	147.04	0.0115	1.0116	0.8690	0.8790	205.90	4.856	0.8990	-13.20
303.15	0.7975	337.17	376.13	157.85	0.0125	1.0126	0.8634	0.9077	150.10	6.662	0.6240	-12.63
308.15	0.7195	363.09	377.60	163.80	0.0134	1.0135	0.8609	0.9745	36.083	27.71	0.152	-9.188
313.15	0.6532	372.01	380.13	170.48	0.0140	1.0141	0.8615	0.9924	10.275	97.31	0.0862	-6.066

*Λ_0 in (S cm^2.mol^{-1}), Λ_m in (S cm^2.mol^{-1}) and ΔG_A in (kJ mol^{-1}).

The enthalpy (HA) for pb(NO$_3$)$_2$ in H$_2$O at various temperature was obtained utilizing Van't Hoff equation (13) [37-38].

$$\log K = -\frac{\Delta H}{2.303R}\left(\frac{1}{T}\right) + \text{constant}$$

(13)

where T is the absolute temperature and R is the gas constant (8.314 J.mole^{-1} degree^{-1}).

The slope of each line, which equals (-ΔH_A/2.303R), can be computed by sketching the relation among log KA and 1/T as illustrated in **Fig. 3.**
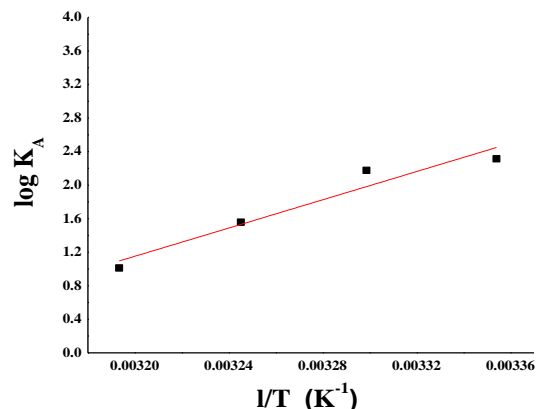
Fig.3: The relationship among Log Ka versus 1/T by kelven for lump pb(NO$_3$)$_2$ in pure water solvent in lack of ligand giving clear difference between them and straight line.

The entropy (ΔS_A) for pb(NO$_3$)$_2$ was determined using the formula (14):

$$\Delta G_A = \Delta H_A - T\Delta S_A \qquad (14)$$

where (S) represents the system's entropy. In **Table 2**, the computed values of (ΔHA) and (ΔSA) for pb(NO$_3$)$_2$ were shown.

Table (2): Entropy change (ΔS_A) and enthalpy change (ΔH_A) of pb(NO$_3$)$_2$ in H$_2$O at various temperatures.

Temperature (K)	Enthalpy change ΔH_A (kJ mol^{-1})	Entropy change ΔS_A (J mol^{-1}K^{-1})
298.15 **303.15** **308.15** **313.15**	-161.266	-0.4965 -0.4985 -0.4935 -0.4878

It was observed that, the association constants for pb(NO$_3$)$_2$ in H$_2$O decrease by increasing temperatures. Also, the free energies of association decrease in negativity indicating less solvation. This was supported an increase in exothermic enthalpies and little difference the case of entropies for lead nitrate salt.

3.1.2. Calculation of association constants and thermodynamic parameters for lead nitrate [pb(NO3)2] with pure water [H2O] in presence of ligand [Orange G, OG].

Experimental measurements were made to determine the specific conductance values (Ks) of various concentrations of pb(NO$_3$)$_2$ in H$_2$O in the presence of OG at different temperatures (298.15,

303.15, 308.15, and 313.15)K. Equation(1) was used to get the values of the molar conductance (Λ_m) .

The limiting molar conductances (Λ_0) for pb(NO$_3$)$_2$ in H$_2$O in the presence of OG were computed by plotting the connections among Λ_m and $C_m^{1/2}$ to zero concentration, as clearly illustrated in Fig. 4.
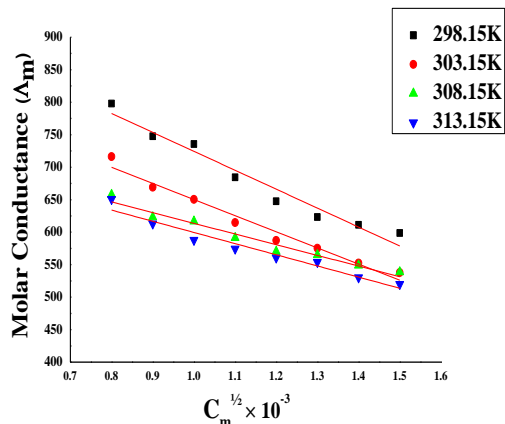
Fig.4: The relationship among molar conductance (Λ_m) and ($C_m^{1/2}$) of pb(NO$_3$)$_2$ in H$_2$O in the existence of OG at various temperatures.

In order to interpret the experimental conductance data, Fuoss-Shedlovsky extrapolation methods, which are based on equation (2-12).

The computed parameters of η_0, Λ_0, Λ, C, $\gamma_\pm$, α ,K$_A$, K$_D$, S, Z, S$_{(Z)}$, K$_3$ and Gibbs free energies for the solutions of pb(NO$_3$)$_2$ in H$_2$O in the presence of OG at various temperatures (298.15, 303.15, 308.15 and 313.15)K were computed and shown in **Table .3.**

Table (3): Various solvation parameters: K$_A$, K$_D$ and K$_3$ for lump pb(NO$_3$)$_2$ in solvent H$_2$O in the presence of OG at varying temperatures.

Tempe rature. (K)	10^2 η_0 (poise)	Λ_m	Λ_0	S	Z	S$_{(z)}$	$\gamma_\pm$	α	K$_A$	10^3 K$_D$	10^5 K$_3$	Δ G$_A$
298.15	0.8 903	735 .50	150 6.50	406 .87	0.0 018	1.0 018	0.9 69	0.4 89	2501 5.59	0.0 39	1.0 74	- 25. 108
303.15	0.7 975	650 .49	127 9.72	364 .69	0.0 019	1.0 019	0.9 68	0.5 09	2220 0.27	0.0 45	0.9 82	- 25. 228
308.15	0.7 195	616 .77	112 0.44	337 .71	0.0 021	1.0 021	0.9 66	0.5 51	1734 5.69	5.7 65	0.8 11	- 25. 012
313.15	0.6 532	587 .89	110 3.53	344 .34	0.0 021	1.0 021	0.9 66	0.5 33	1924 3.04	5.1 96	0.8 80	- 25. 688

Λ_0 in (S cm^2.mol^{-1}), Λ_m in (S cm^2.mol^{-1}) and ΔG$_A$ in (kJ mol^{-1}).

The enthalpy (ΔH_A) of pb(NO$_3$)$_2$ in H$_2$O in the presence of OG at various temperatures were determined using a Van't Hoff formula (13).

The slope of each line equals (-ΔHA/2.303R) when the relationship between log KA and 1/T is drawn and calculating ΔHA is possible.as illustrated in **Fig. 5** . The entropy (ΔS_A) for pb(NO$_3$)$_2$ was calculated by using equation (14). The computed parameters of (ΔH_A) and (ΔS_A) for pb(NO$_3$)$_2$ were presented in **Table.4.**
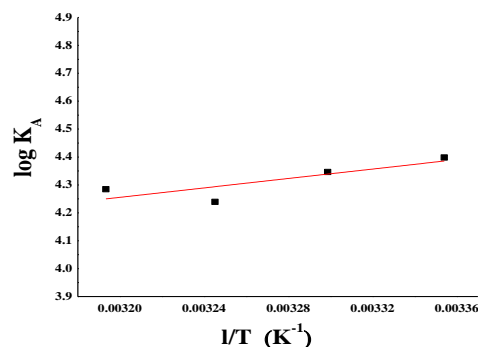
Fig.5: The relationship among Log Ka versus 1/T by kelven for lump pb(NO$_3$)$_2$ with OG in H$_2$O.

Table (4): Entropy change (ΔS_A) and enthalpy change (ΔH_A) of pb(NO$_3$)$_2$ involving OG in H$_2$O at various temperatures.

Temperature. (K)	Enthalpy change ΔH_A (kJ mol^{-1})	Entropy change ΔS_A (J mol^{-1}K^{-1})
298.15 **303.15** **308.15** **313.15**	-16.162	0.0300 0.0299 0.0287 0.0304

It was observed that, the association thermodynamic parameters for solvation are greater for pb(NO$_3$)$_2$ with OG than that of pb(NO$_3$)$_2$ alone favoring more ion-solvent interaction. More Gibbs free energies values were observed and increased by increasing temperatures indicating mors spontaneous reaction between pb(NO$_3$)$_2$ with OG in pure water.Also, enthalpies and entropies for pb(NO$_3$)$_2$ with OG in pure water indicating more aggregation of lead ions with OG in solutions.

3.1.3. Determination of the thermodynamic parameters and formation constants for lead nitrate [pb(NO$_3$)$_2$] with pure water [H$_2$O] in presence of ligand [Orange G, OG].

Experimental measurements of the specific conductance values (Ks) of various concentrations for pb(NO$_3$)$_2$ in H$_2$O were made when the orange G are together at various temperatures (298.15, 303.15,

308.15, and 313.15)K. Equation (1) was used to calculate the molar conductance (Λ_m) values .

By plotting the relationship between the molar conductance (Λ_m) for pb(NO$_3$)$_2$ in the existence of OG at varying temperatures and the molar ratio of metal to ligand [M]/[L] concentrations, various lines with breaks were discovered, showing the development of 1:2 and 1:1 (M:L) stoichiometric complexes in Fig. 6.
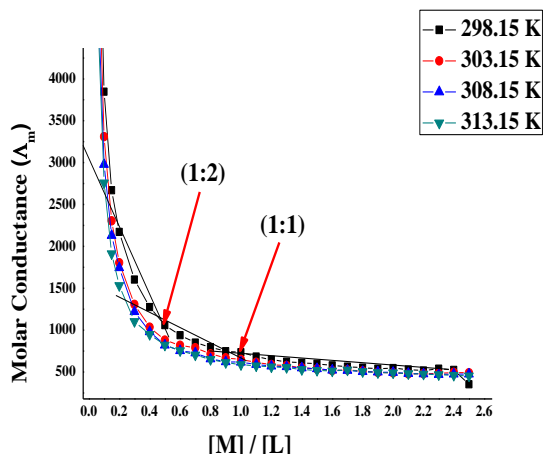
Fig.6: The relation between the molar conductance Λ_m against [M]/[L] of pb(NO$_3$)$_2$ involving OG in H$_2$O at different temperatures.

The formation constants (K_f) for pb(NO$_3$)$_2$ complexes were computed for each type of complexes (1:2) and (1:1) (M:L) by utilising a formula. (15) [39-42].:

$$K_f = \frac{[ML]}{[M][L]} = \frac{\Lambda_{M-}\Lambda_{obs}}{(\Lambda_{obs-}\Lambda_{ML})[L]} \qquad (15)$$

$$[L] = [L]_t - [M]_t \frac{(\Lambda_M - \Lambda_{Obs})}{(\Lambda_{Obs} - \Lambda_{ML})}$$

where [L] is the concentration of the ligand, OG, and [Λ_M] is the limiting molar conductance of pb(NO3)2 alone, [obs] is the molar conductance of the solution during titration, [Λ_{ML}] is the molar conductance of the complex, and [Λ_{obs}] is the molar conductance of the system as a whole.

Equation (16) was used to determine the Gibbs free energy of production for each molar ratio complex (ΔGf).

$$\Delta G_f = - 2.303 \ RT \ log \ K_f \qquad (16)$$

Table 5 shows the calculated ΔGf values for the pb(NO$_3$)$_2$ stoichiometric complexes as well as the actual values (Kf).

Table (5): formation thermodynamic parameters for complex formation for 1:2 and 1:1 (M/L) of pb(NO$_3$)$_2$ with OG in H$_2$O at different temperatures.

Complexity proportion (M:L)	Temperature (K)	log K$_f$	ΔG$_f$
(1:2)	298.15 303.15 308.15 313.15	2.19 4.11 4.12 3.82	-12.50 -23.87 -24.29 -22.93
(1:1)	298.15 303.15 308.15 313.15	4.184 3.967 3.916 4.075	-23.88 -23.03 -23.11 -24.43

Different lines were generated by scheming the relationship of log Kf against 1/T, demonstrating the production of the molar ratio combinations 1:2 and 1:1 (M:L) **Fig7.**
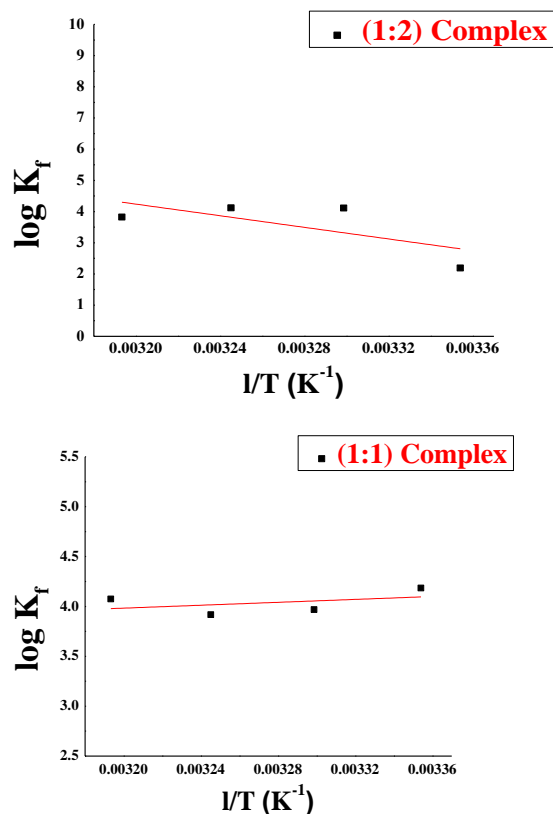
Fig.7: A different version of log K**f** against 1/T (K^{-1}) for (a) (1:2) complex (b) (1:1) complex of pb(NO$_3$)$_2$ with OG in H$_2$O.

For each type of complex, Hf may be determined from the relationship among log Kf and 1/T using the slope of each line, which equals $(-\Delta Hf/2.303R)$. Equation (17) was used to determine the entropy (ΔSf) for $pb(NO_3)_2$ stoichiometric complexes of the classes (1:2) and (1:1) (M:L).

$$\Delta G_f = \Delta H_f - T\Delta S_f \qquad (17)$$

The computed parameters of (ΔH_f) and (ΔS_f) of $pb(NO_3)_2$ molar ratio complexes were displayed in **Table.6.**

Table (6): Entropy change (ΔS_f) and enthalpy change (ΔH_f) of formation of $pb(NO_3)_2$ involving OG complexes in H_2O at multiple temperatures.

[M:L] complex	ΔH_f (kJ mol^{-1})	ΔS_f (J mol^{-1} K^{-1})			
		298.15 K	303.15 K	308.15 K	313.15 K
(1:2)	178.11	0.6393	0.6663	0.6568	0.6419
(1:1)	-13.98	0.0332	0.0298	0.0296	0.0334

It was found that the development of from both molar ratio combinations in the solutions was indicated by inflections at (1:1) M/L and (1:2) M/L proportions. The interactions of $pb(NO_3)_2$ and OG in pure water at various temperatures resulted in the formation of several kinds of stoichiometric complexes. Complexes with a 1:1 ratio have better complex formation properties than those with a 1:2 ratio, indicating that they are more advantageous.

Additionally, as temperatures rose due to an increase in kinetic energy, the complex formation parameters (Kf, ΔGf) increased as well.

3.2. Molecular docking

Multiple possible adduct structures produced by molecular docking were scored and categorized using the software's scoring function. It is possible to infer the binding energy, free energy, and stability of Orange G and its lead complex using the knowledge obtained through the docking method [43–46].

In order to examine the binding interactions and conformation structure that contribute to the relationship among proteins and compounds, molecular docking has been applied to Orange G and its lead complex with the crystal structure of human prostate specific antigen (PSA) in Fab sandwich with a high affinity and a PCa selective antibody (3QUM). **Fig.8 (a,b)**.

From the docking we predict that strong interactions between the inhibitor (Orange G Lead complex) and the active site coupled to chain (p) of (3QUM)and its energy content (-6.4417 kcal mol^{-1}) compared with (Orange G) whose energy value (-5.8964 kcal mol^{-1}), **Table.7 (a, b)**.

The prostate cancer protein PC3 (PDB = 3QUM) interacted via amino acid pocket molecules with Orange G through O15 by accepting H atoms with ARG amino acid receptors, **Table. 8 (a)**. While interacted with Orange G Lead complex via O 34, O 36, and O 38 by accepting H atoms with GLY 19 and LYS 154 amino acid receptors, **Table. 8(b)**. In vitro inhibitory activities are shown by greater engagement among substances and receptors.
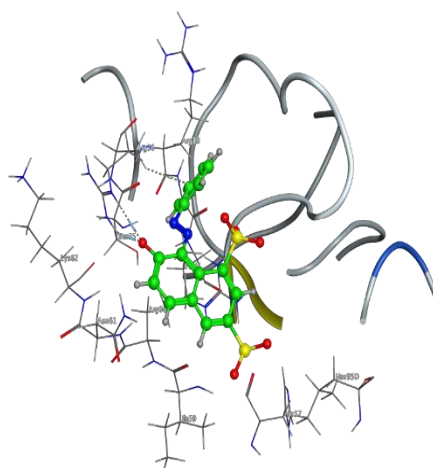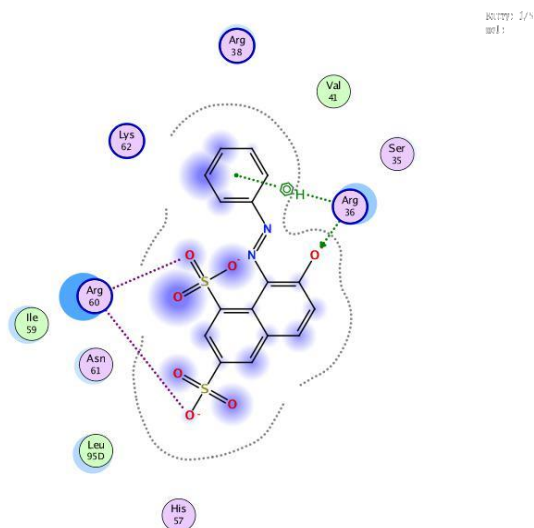
Fig.8(a): 2D and 3d diagram exhibit the interaction among Orange G and active sites of 3QUM protein.

_____
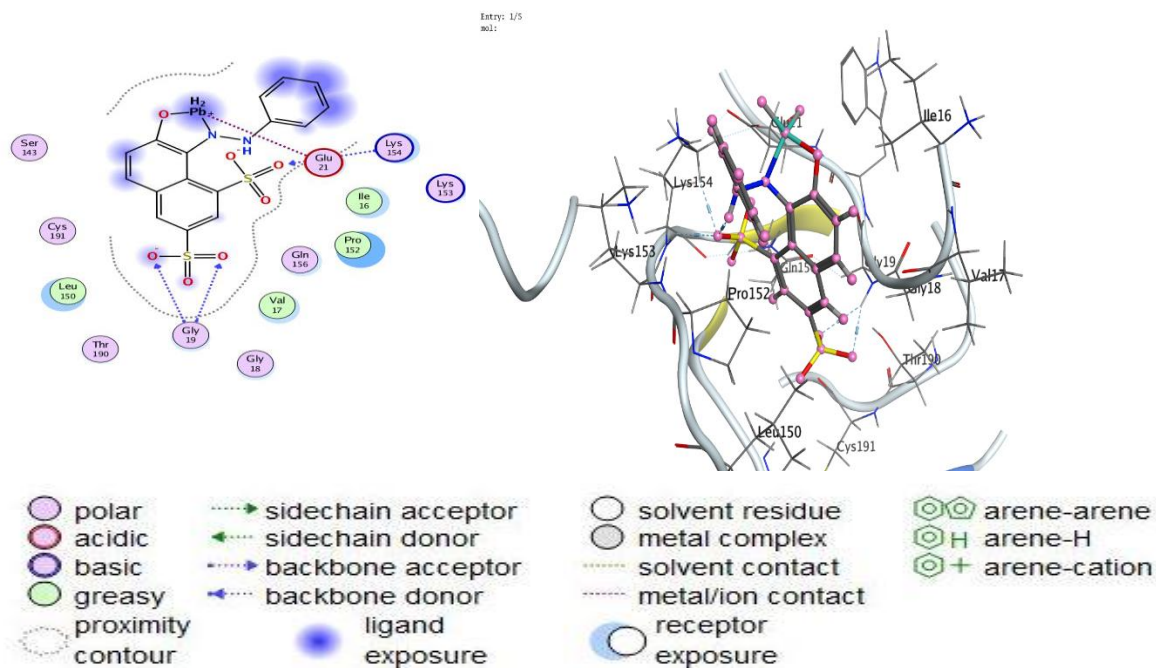
Fig.8(b): Diagrams in two-dimensional and three-dimensional exhibit the Communication among Orange G lead complex and the 3QUM protein's functional areas.

Table.7 (a): The ideal configurations of Orange G within the protein's active region

Molecule.	mseq	S	rmsd_refne	E_conf	E_place	E_score1	E_refne	E_score2
	1	-5.8964	1.4755	-85.1062	-37.2946	-10.8325	-35.5977	-5.8964
	1	-5.8298	1.6586	-89.0871	-57.6456	-11.5905	-35.1803	-5.8298
	1	-5.1721	2.0747	-91.2260	-41.0650	-10.5607	-26.8877	-5.1721
	1	-5.1050	2.2596	-89.0788	-52.0922	-10.3782	-26.8580	-5.1050
	1	-5.1042	2.7472	-86.3499	-28.3195	-11.3068	-34.3243	-5.1042
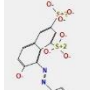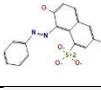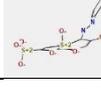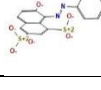
_____

Table.7(b): The Orange G lead complex in its greatest potential conformations inside the protein's active region.
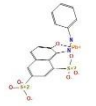
Molecule.	mseq	S	rmsd_refne	E_conf	E_place	E_score1	E_refne	E_score2
	1	-6.4417	2.4213	19.3752	-31.1989	-9.7684	-34.7274	-6.4417
	1	-6.0692	2.0984	31.9305	-76.7421	-9.8671	-25.4621	-6.0692
	1	-5.8262	1.2956	6.4925	-52.2826	-9.8281	-29.6559	-5.8262
	1	-5.7993	2.0573	9.9972	-41.8141	-12.4307	-28.9489	-5.7993
	1	-5.7858	1.9588	9.0578	-58.4622	-10.7249	-30.2520	-5.7858
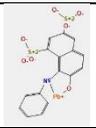
Table.8 (a): Orange G Connection with the 3QUM Protein

Ligand	Receptor	Communication	Distance	E (kcal/mol)
O 15	NE ARG 36 (P)	H- acceptor	3.10	-4.1
O 15	NH2 ARG 36 (P)	H- acceptor	2.83	-6.7
6-ring	CB ARG 36 (P)	Pi-H	4.03	-0.7

Table.8 (b): Orange G lead complex Connection with the 3QUM Protein

Ligand	Receptor	Communication	Distance	E (kcal/mol)
O 34	N GLY 19 (P)	H- acceptor	3.13	-2.0
O 36	N GLY 19 (P)	H- acceptor	3.29	-2.1
O 38	N LYS 154 (P)	H- acceptor	3.34	-1.5
O 38	CE LYS 154 (P)	H- acceptor	3.16	-2.1

4. Conclusion

1. Complex thermodynamic parameters for bulk associations for $Pb(NO_3)_2$ in presence of Orange G were also determined by the conductance measurements method in a water solvent.

2. From the conductometric data was observed that two stoichiometric complexes were obtained 1:1 and 1:2 ($Pb(NO_3)_2$/ Orange G) from the interaction of $Pb(NO_3)_2$ with fuchsin acid .

3. In the case of 1:1 as compared to 1:2, the complex thermodynamic formation parameters Kf and Gf are larger. ($Pb(NO_3)_2$/ Orange G) complexes for bulk in water solvent.

4. Finally , Orange G and its lead complex with the crystalline structure for the human prostate-specific antibody (PSA) in a Fab sandwich have been subjected to molecular docking with a high affinity. Utilizing Docking Server software, molecular modelling and computational computations were completed.

5. References

[1] C. P. Kelly, C.J Cramer, D. G. Truhlar, J. (Chem. Theory Comput., 1 (2005) 1133.
[2] D.Yaffe,Y.Cohen, G. Espinosa, A. Arenas, F. Giralt, 1. Chem. Inf. Compt.Sci.43 (2003) 85.

[3] N. A. Izmailov, Russ. J. Phys. Chem., 34 (1960) 1142.

[4] M. Hakimi, A. Nezhadali, A. Naemi, Conductometric study ofcomplex formation between Cu(II) ion and 4-amino-3-ethyl-1,2,4-triazol-5-thione in binary ethanol/water mixtures, E-J.Chem. 5 (2008) 551–556.

[5] A. Nezhadali, Gh. Taslimi, Thermodynamic study of complex formation between 3,5-di iodo-hydroxyquinoline and Zn^{2+}, Ni^{2+} and Co^{2+}cations in some binary solvents using a conductometric method, Alexandria Engineering Journal (2013) 52, 797–800.

[6] R.G. Ding, G.Q. Lu, Z.F. Yan, M.A. Wilson, Journal of Nanoscience and Nanotechnololgy (2001) 1: pp. 1-23.

[7] D. F. Evans, Sister Marry, A. Matesich, Electro Chemistry, Ed. E. Yeager, A.J. Salkind, John-Wiley and Sons, 2 (1973) Chapter 1.

[8] Gray, James R. "Conductivity Analyzers and Their Application". In Down, R.D; Lehr, J.H. Environmental Instrumentation and Analysis Handbook, Wiley (2004) pp. 491–510

[9] Schröer, W.; Weingärtner, H. (2004). "Structure and criticality of ionic fluids".Pure Appl. Chem. 76 (1): 19–27.

[10] R.K. Christopher, A. Glasson, L.F. Lindoy, V. George, M. Meehana, Developments in the d-block metallo-supramolecular chemistry of polypyridyls, Coor. Chem. Rev. 252 (2004) 940–948.

[11] M. Fainerman-Melnikova, A. Nezhadali, Gh. Rounaghi, C. Mcmurtrie, J. Kim, J. Gloe, K. Langer, S.S. Lee, L.F. Lindoy, T. Nishimur, M.K. Park, L.L. Seo, Metal ion recognition via selective detuning. The interaction of selected transition and posttransition metal ions with a mono-N-benzylated O2N3-donor macrocycle and its xylyl- bridged ring analogue, J. Chem. Soc. Dalton Trans. (2004) 122–128.

[12] A. Nezhadali, N. Rabani, Competitive bulk liquid membrane transport of Co(II), Ni(II), Zn(II), Cd(II), Ag(I), Cu(II) and Mn(II), cations using 2,20-dithio (bis) benzothiazole as carrier, Chin. Chem. Lett. 22 (2011) 88–92.

[13]- M. Xie, L. Gao, L. Li, W. Liu, S. Yan, J. Inorg. Biochem. 99 (2005) 546–551.

[14]- A. Sheela, R. Vijayaraghavan, J. Coord. Chem. 64 (2011) 511.

[15]- Y. Wei, C. Chan, J. Tian, G. Jang, K.F. Hsueh, Electrochemical Polymerization of Thiophenes in the Presence of Bithiophene or Terthiophene : Kinetics and Mechanism of the Polymerization *Chemistry of Materials*, (1991) 888–897.

[16]- S.N. Haier, S. Park, Electrochemistry of Conductive Polymers, *Journal of the Electrochemical Society*. 140 (1993) 2454–2463.

[17] J. Wang, J.D. MacNEIL, J.F. Kay (2012), John Wiley. (2012) P. 464.

[18] C.L. Hsueh, Y.H. Huang, C.C. Wang, C.Y. Chen, Degradation of azo dyes using 385 low iron concentration of Fenton and Fenton-like system, Chemosphere 58 (2005) 386 1409–1414

[19] J.H. Sun, X.L. Wang, J.Y. Sun, R.X. Sun, S.P. Sun, L.P. Qiao, Photocatalytic 424 degradation and kinetics of Orange G using nano-sized Sn(IV)/TiO2/AC 425 photocatalyst, J. Mol. Catal. A: Chem. 260 (2006) 241–246. 426

[20] S.P. Sun, C.J. Li, J.H. Sun, S.H. Shi, M.H. Fan, Q. Zhou, Decolorization of an azo 427 dye Orange G in aqueous solution by Fenton oxidation process: Effect of system 428 parameters and kinetic study, J. Hazard Mater. 161 (2009) 1052–1057.

[21] Bikadi Z., Hazai E., Cheminformatics. J., 1 (2009) 1–16.

[22] Halgren T.A., Merck Molecular Force Field., 11(17) (2000) 520–552.

[23] A.I. Vogel, Quantitative Inorganic Analysis, Longmans, London, (1989).

[24] A.I. Popov and J.M. Lehn, in: G.A. Melson (Ed.), Coordination Chemistry of Macrocyclic Compounds, Plenum press, New York (1985).

[25] R.D. Lillie "The hematoxylin shortage and the availability of synthetic substitutes". *Am J Med Technol.* 40 (11): 455–61(1974).

[26] Carson, L. Freida; Hladik, Christa; Histotechnology: A Self-Instructional Text (3 ed.). *Hong Kong:American Society for Clinical Pathology Press.* p.362. (2009).

[27] Bancroft, John; Stevens, Alan, eds. "The Theory and Practice of Histological Techniques" (2nd ed.). Longman Group Limited (1982).

[28] A.I. Popov, *Pure Appl. Chem.* 51 (1979) 101–105.

[29] W. Gryzybkowski and R. Pastewski; *Electrochimica Acta*; (1980) 25, 279.

[30] A.A.El-Khouly, E.A. Gomaa and S.E.Salem ; *South, Braz. J. Chem.*20 (2012).

[31] E. A. Gomaa, E. M. Abou El-Leef, K. S. Shalaby, S. E. Salem; *Journal of Environments,* 2014, 1(2): 44-53.

[32] T.Shdlovsky and R.L. Kay ; *J.Phys., Chem.* 60 (1956) 151.

[33] E.Hirsch and R.M.Fuoss ; *J. Amer. Chem. Phys.*, 25 (1956)1199.

[34] E. M. Abouelleef1, E. A. Gomaa, S. E. Salem*; American Journal of Chemistry and Application,* 2015; 2(1): 1-11

[35] R. M. Fuoss and F. Accascina ; Electrolytic conductance, Interscience, New York (1959).

[36] O.Popuych, A.Gibofsky and D.H. Berne ; *Analytic. Chem.*, 44(1972)811.

[37] Isabel, M. S. Lampreia, L. and A.V. Ferreira, *J. Chem. Soc. Faraday. Trans. T.*, 92 (1996) 1487.

DIFFERENT STUDIES ON THE INTERACTION OF LEAD NITRATE SALT WITH ORANGE G..

367

[38] P.W. Atkins; Physical chemistry; Oxford University Press (1978).

[39] D.J.G. Ives; Chemical Thermodynamics, University Chemistry, Macdonald Technical and Scientific, London (1971).

[40] Y. Takeda; *Bull. Chem. Soc. Jpn* (1983) 56,3600.

[41] M. R. Nasrabadi, F. Ahmadi, S.M. Pourmortazavi, M.R. Ganjali and K. Alizadeh; *Journal of Molecular Liquids*; 144 (2009) 97–101.

[42] Y.Takeda, *Bull. Chem. Soc. Jpn.* 56, 3600–3602 (1983).

[43] M. Dar, S. Mir, *J. Anal Bioanal Tech* (2017), 8:2.

[44] D. B. Kitchen, H. Decornez, J.R. Furr, J. Bajorath, *Drug Discovery* (2004), 3, 935-949.

[45] A.N.Jain "Scoring functions for protein-ligand docking" *Curr. Protein Pept. Sci.* 7(5), 407–420 (2006)

[46] M. Zheng, B. Xiong, C. Luo ; *J. Chem. Inf. Model.* 51(11), 2994–3004 (2011).